Generalized Continua and Size Effects in Elastostatic Bending Experiments

Christian Liebold, Wolgfang H. Müller
Christian.Liebold@TU-Berlin.de

Abstract

In this work we deal with a finite element approach to the modified strain gradient theory, which will be used to describe size dependent material behavior within the framework of an elastic theory. The couple stress-, strain gradient-, and material surface theories are analyzed in context with beam bending. The derivation of a variational formulation of the modified strain gradient theory is presented and implemented in an open-source FE-environment for solution. By using an atomic force microscope to record force and deflection data of micro-cantilevers made of the material epoxy, a size effect is revealed and higher-order material coefficients could be measured and obtained.

Introduction

Driven by miniaturization and by the quest for reducing the costs of materials the simulation and the valuation of reliability of engineering materials grows in importance. Size effects in elasticity need to be accounted for, either in a physically detailed manner, or as an alternative technique of homogenization. Materials with intrinsic micro- or nano-structure may show size-dependent material behavior, which is reflected by a stiffer or softer elastic response to external forces when the size of the material body is reduced. This has been observed in several experiments on metals and polymers, for example, in copper [8], silver [15], zinc oxide [21], lead [4], carbon nanotubes [20], epoxy [3] and polypropylene [16]. Conventional (Cauchy-) continuum theory is unable to predict size effects. Several continua of higher order were proposed in the literature, such as *non-local theories* [7], *strain gradient theories* [18], *micropolar theories* [5, 19], *theories of material surfaces* [10] or *fractional continuum mechanics* [2].

1 Some continuum mechanical theories of higher order

With respect to size effects we distinguish between micromorphic and strain gradient theories [7] as an extension to the conventional Cauchy continuum. Additionally,

the theory of elastic material surfaces [10] is taken into account. The origin of generalized continua is detailed in [1]. By quoting ERINGEN (*cf.* [6], pp. 33) we may state that "a *micromorphic continuum* may be thought of as a classical continuum to each point of which is associated another continuum." The additional continuum, thought as a continuous distribution of deformable point particles, is restricted to homogeneous deformations[1]. The intrinsic deformation of the point particles is described by directors, which are first-order tensors "attached" to each material point. A second-order tensor Q_{ij} maps the particle's orientation and deformation between different configurations. In the special case of a *micropolar continuum*, Q_{ij} is an arbitrary proper orthogonal tensor. The point particles are restricted to rotations only. In the Couple Stress-, or pseudo-COSSERAT continuum (CS), the rotational degree of freedom φ_i of the associated continuum is related to the macroscopic rotation vector $\frac{1}{2}\epsilon_{ijk}u_{k,j}$, where use is made of the summation convention on repeated indices. In what follows comma separated indices denote partial spatial derivatives with respect to a Cartesian coordinate system defined in the current frame.
The theory of material surfaces, a.k.a. *Surface Elasticity* (SE), captures surface characteristics that may differ from those of the volume. For example, these differences are caused by surface oxidation, aging, coating, atomic and molecular rearrangement or even surface roughness. Discrete formulae for the problem of simple beam bending are given, using the EULER-BERNOULLI assumptions for the displacement field u_i. From these relations, generalized elastic moduli for isotropic materials of the CS- and SE theory read [22, 17]:

$$E_{\mathrm{CS}} = E\left(1 + 6\frac{\ell^2}{T^2}\right), \quad E_{\mathrm{SE}} = E + E^{\mathrm{surf}}\left(\frac{6}{T} + \frac{2}{W}\right), \tag{1}$$

where E denotes the conventional YOUNG's modulus, and T the thickness of beams with rectangular cross-sections, W being their width, and ℓ, as well as E^{surf} the corresponding additional material parameters of the underlying higher order theory.

In contrast to micromorphic continua and to the theory of material surfaces, the idea behind *Strain Gradient theories* (SG) is the extension of the kinematic variables by defining second order derivatives of the displacement vector, without introducing additional degrees of freedom. Hence, the gradient of the small strain tensor $\tilde{\eta}_{ijk} = \varepsilon_{kj,i}$ is used explicitly in the strain energy density u and it is connected to stress measures as follows [18]:

$$u^{\mathrm{SG}} = u(\varepsilon_{ij}, \tilde{\eta}_{ijk}) \ , \quad \sigma_{ij} = \frac{\partial u^{\mathrm{SG}}}{\partial \varepsilon_{ij}} \ , \quad \mu_{ijk} = \frac{\partial u^{\mathrm{SG}}}{\partial \tilde{\eta}_{ijk}} \ , \tag{2}$$

where σ_{ij} denotes the CAUCHY stress tensor and μ_{ijk} the higher-order stress tensors.

2 The Modified Strain Gradient theory (MSG)

The decomposition of $\tilde{\eta}_{ijk}$ in combination with utilizing the macroscopic rotation vector φ_i results in a reduction of independent additional material parameters from five down to three. FLECK & HUTCHINSON (1997) [9] first introduced independent

[1]The displacement gradient is constant for the (sub-)body.

metrics of $\eta_{ijk} = u_{k,ij}$ and decomposed the second order displacement gradient into its symmetric and anti-symmetric part, $\bar{\bar{\eta}}_{ijk}$ and η^{A}_{ijk}:

$$\bar{\bar{\eta}}_{ijk} = \tfrac{1}{3}\left(u_{k,ij} + u_{i,jk} + u_{j,ki}\right) \ , \quad \eta^{\mathrm{A}}_{ijk} = \tfrac{2}{3}\left(\epsilon_{ikl}\bar{\eta}_{lj} + \epsilon_{jkl}\bar{\eta}_{li}\right) \ , \tag{3}$$

where $\bar{\eta}_{ij} = \varphi_{i,j}$ is the gradient of rotation (decomposed into its symmetric and anti-symmetric part, χ^{S}_{ij} and χ^{A}_{ij} as well):

$$\bar{\eta}_{ij} = \tfrac{1}{2}\epsilon_{ilk}u_{k,lj}\,, \quad \varphi_i = \tfrac{1}{2}\epsilon_{ilk}u_{k,l}\,, \quad \chi^{\mathrm{A}}_{ij} = \tfrac{1}{2}\left(\varphi_{i,j} - \varphi_{j,i}\right), \quad \chi^{\mathrm{S}}_{ij} = \tfrac{1}{2}\left(\varphi_{i,j} + \varphi_{j,i}\right), \tag{4}$$

ϵ_{ilk} being the alternating tensor (Levi-Civita symbol). $\bar{\bar{\eta}}_{ijk}$ is further decomposed into its spherical and deviatoric parts, $\eta^{(0)}_{ijk}$ and $\eta^{(1)}_{ijk}$. $\eta^{(0)}_{ijk}$ is related to χ^{A}_{ij} and the dilatation gradient $\varepsilon_{mm,i}$ in the following manner [9]:

$$\eta^{(0)}_{ijk} = \tfrac{1}{5}(\delta_{ij}\bar{\bar{\eta}}_{mmk} + \delta_{jk}\bar{\bar{\eta}}_{mmi} + \delta_{ki}\bar{\bar{\eta}}_{mmj}) \ , \quad \bar{\bar{\eta}}_{mmi} = \varepsilon_{mm,i} + \tfrac{2}{3}\epsilon_{iln}\chi^{\mathrm{A}}_{ln} \ . \tag{5}$$

By assuming symmetry of the couple stress tensor μ_{ij}, the anti-symmetric part of the gradient of rotation does not influence the strain energy, as shown in [13, 22]. A linear strain energy density for nonsimple isotropic materials of the modified gradient type reads:

$$u^{\mathrm{MSG}} = \hat{u}(\varepsilon_{ij}\,, \varepsilon_{mm,i}\,, \eta^{(1)}_{ijk}\,, \chi^{\mathrm{S}}_{ij}) = \tfrac{1}{2}\sigma_{ij}\varepsilon_{ij} + \tfrac{1}{2}p_i\varepsilon_{mm,i} + \tfrac{1}{2}\mu^{(1)}_{ijk}\eta^{(1)}_{ijk} + \tfrac{1}{2}\mu_{ij}\chi^{\mathrm{S}}_{ij} \ , \tag{6}$$

and the corresponding work-conjugated stress measures are:

$$\begin{aligned} \sigma_{ij} &= \frac{\partial u^{\mathrm{MSG}}}{\partial \varepsilon_{ij}} = \lambda\varepsilon_{kk}\delta_{ij} + 2\mu\varepsilon_{ij} \ , & p_i &= \frac{\partial u^{\mathrm{MSG}}}{\partial \varepsilon_{nn,i}} = 2\mu\ell_0^2\varepsilon_{mm,i} \\ \mu^{(1)}_{ijk} &= \frac{\partial u^{\mathrm{MSG}}}{\partial \eta^{(1)}_{ijk}} = 2\mu\ell_1^2\eta^{(1)}_{ijk} \ , & \mu_{ij} &= \frac{\partial u^{\mathrm{MSG}}}{\partial \chi^{\mathrm{S}}_{ij}} = 2\mu\ell_2^2\chi^{\mathrm{S}}_{ij} \ . \end{aligned} \tag{7}$$

λ and μ are Lamé's constants, whereas $\ell_0 = \ell_1 = \ell_2 = \ell$ denote the additional material length scale parameters, which are chosen to be equal to ℓ without providing further arguments.

3 Finite element approach

A solution strategy for the modified strain gradient theory is presented using finite elements in context with the open-source FE-project FEniCS©, [14]. It allows to directly implement variational formulations of partial differential equations.

3.1 Variational formulation of MSG theory

The starting point is the local form of the equilibrium equation of the linear momentum of MSG theory, given by [12]:

$$\sigma_{ik,i} - p_{i,ik} - \mu^{(1)}_{ijk,ij} - \tfrac{1}{2}\epsilon_{jlk}\mu_{ij,il} + f_k = \rho\ddot{u}_k \ . \tag{8}$$

The variational formulation of the strain energy in a global formulation results after multiplication of an arbitrary first-order tensor function for displacements (so-called test function) δu_k:

$$\int_V \left(\sigma_{ik,i}\delta u_k - p_{i,ik}\delta u_k - \mu^{(1)}_{ijk,ij}\delta u_k - \tfrac{1}{2}\epsilon_{jlk}\mu_{ij,il}\delta u_k\right)\mathrm{d}V = 0 \ , \tag{9}$$

where the body-force vector f_k is set to be equal to zero and static conditions are assumed. In view of the so-called test function u_k, Eqn. (9) represents a partial differential equation of fourth order. Reduction from fourth-order to a third-order differential equation is achieved by applying, first, the product rule for differentiation to each summand:

$$\begin{aligned}
\int_V \sigma_{ik,i}\delta u_k \mathrm{d}V &= \int_V \left(\sigma_{ik}\delta u_k\right)_{,i}\mathrm{d}V - \int_V \sigma_{ik}\delta u_{k,i}\mathrm{d}V \ , \\
\int_V p_{i,ik}\delta u_k \mathrm{d}V &= \int_V \left(p_{i,i}\delta u_k\right)_{,k}\mathrm{d}V - \int_V p_{i,i}\delta u_{k,k}\mathrm{d}V \ , \\
\int_V \mu^{(1)}_{ijk,ij}\delta u_k \mathrm{d}V &= \int_V \left(\mu^{(1)}_{ijk,i}\delta u_k\right)_{,j}\mathrm{d}V - \int_V \mu^{(1)}_{ijk,i}\delta u_{k,j}\mathrm{d}V \ , \\
\int_V \tfrac{1}{2}\epsilon_{jlk}\mu_{ij,il}\delta u_k \mathrm{d}V &= \int_V \left(\tfrac{1}{2}\epsilon_{jlk}\mu_{ij,i}\delta u_k\right)_{,l}\mathrm{d}V - \int_V \tfrac{1}{2}\epsilon_{jlk}\mu_{ij,i}\delta u_{k,l}\mathrm{d}V \ ,
\end{aligned} \tag{10}$$

and, second, Gauss' theorem to transform volume into surface integrals:

$$\begin{aligned}
\int_V \sigma_{ik,i}\delta u_k \mathrm{d}V &= \oint_{\partial V} \sigma_{ik}\delta u_k n_i \mathrm{d}A - \int_V \sigma_{ik}\delta u_{k,i}\mathrm{d}V \ , \\
\int_V p_{i,ik}\delta u_k \mathrm{d}V &= \oint_{\partial V} p_{i,i}\delta u_k n_k \mathrm{d}A - \int_V p_{i,i}\delta u_{k,k}\mathrm{d}V \ , \\
\int_V \mu^{(1)}_{ijk,ij}\delta u_k \mathrm{d}V &= \oint_{\partial V} \mu^{(1)}_{ijk,i}\delta u_k n_j \mathrm{d}A - \int_V \mu^{(1)}_{ijk,i}\delta u_{k,j}\mathrm{d}V \ , \\
\int_V \tfrac{1}{2}\epsilon_{jlk}\mu_{ij,il}\delta u_k \mathrm{d}V &= \oint_{\partial V} \tfrac{1}{2}\epsilon_{jlk}\mu_{ij,i}\delta u_k n_l \mathrm{d}A - \int_V \tfrac{1}{2}\epsilon_{jlk}\mu_{ij,i}\delta u_{k,l}\mathrm{d}V \ .
\end{aligned} \tag{11}$$

The reduction from a third-order to a second-order differential equation is achieved by a second manipulation of this kind to Eqns. $(11)_2$, $(11)_3$ and $(11)_4$:

$$\begin{aligned}
\int_V p_{i,i}\delta u_{k,k}\mathrm{d}V &= \oint_{\partial V} p_i \delta u_{k,k} n_i \mathrm{d}A - \int_V p_i \delta u_{k,ki}\mathrm{d}V \ , \\
\int_V \mu^{(1)}_{ijk,i}\delta u_{k,j}\mathrm{d}V &= \oint_{\partial V} \mu^{(1)}_{ijk}\delta u_{k,j} n_i \mathrm{d}A - \int_V \mu^{(1)}_{ijk}\delta u_{k,ji}\mathrm{d}V \ , \\
\int_V \tfrac{1}{2}\epsilon_{jlk}\mu_{ij,i}\delta u_{k,l}\mathrm{d}V &= \oint_{\partial V} \tfrac{1}{2}\epsilon_{jlk}\mu_{ij}\delta u_{k,l} n_i \mathrm{d}A - \int_V \tfrac{1}{2}\epsilon_{jlk}\mu_{ij}\delta u_{k,li}\mathrm{d}V \ .
\end{aligned} \tag{12}$$

We now insert Eqns. (11) and (12) into (9) and separate volume from surface integrals:

$$
\begin{aligned}
&-\int_V \left(\sigma_{ik}\delta u_{k,i} + p_i\delta u_{k,ki} + \mu^{(1)}_{ijk}\delta u_{k,ji} + \tfrac{1}{2}\epsilon_{jlk}\mu_{ij}\delta u_{k,li}\right)\mathrm{d}V = \\
&\oint_{\partial V}\left(-\sigma_{ik}n_i\delta u_k + p_{i,i}n_k\delta u_k + \mu^{(1)}_{ijk,i}n_j\delta u_k + \tfrac{1}{2}\epsilon_{jlk}\mu_{ij,i}n_l\delta u_k\right)\mathrm{d}A - \\
&\qquad\oint_{\partial V}\left(p_i n_i\delta u_{k,k} + \mu^{(1)}_{ijk}n_i\delta u_{k,j} + \tfrac{1}{2}\epsilon_{jlk}\mu_{ij}n_i\delta u_{k,l}\right)\mathrm{d}A\ .
\end{aligned}
\tag{13}
$$

We identify the resulting boundary conditions for the surface-traction vector $\bar{t}_k$:

$$
\begin{aligned}
&\oint_{\partial V}\left(\sigma_{ik}n_i - p_{i,i}n_k - \mu^{(1)}_{ijk,i}n_j - \tfrac{1}{2}\epsilon_{jlk}\mu_{ij,i}n_l\right)\delta u_k\mathrm{d}A = \\
&\qquad\oint_{\partial V}\underbrace{\left(\sigma_{ik} - p_{j,j}\delta_{ik} - \mu^{(1)}_{lik,l} - \tfrac{1}{2}\epsilon_{jik}\mu_{lj,l}\right)n_i}_{\bar{t}_k}\delta u_k\mathrm{d}A\ ,
\end{aligned}
\tag{14}
$$

the surface double-traction tensor $\bar{m}_{jk}$, as well as the surface dilatation vector $\bar{p}_i$:

$$
\begin{aligned}
&\oint_{\partial V}\left(p_i n_i\delta u_{k,k} + \mu^{(1)}_{ijk}n_i\delta u_{k,j} + \tfrac{1}{2}\epsilon_{jlk}\mu_{ij}n_i\delta u_{k,l}\right)\mathrm{d}A\ = \\
&\oint_{\partial V}\underbrace{p_i}_{\bar{p}_i}n_i\delta u_{k,k}\mathrm{d}A + \oint_{\partial V}\underbrace{\left(\mu^{(1)}_{ijk} + \tfrac{1}{2}\epsilon_{ljk}\mu_{il}\right)n_i}_{\bar{m}_{jk}}\delta u_{k,j}\mathrm{d}A\ .
\end{aligned}
\tag{15}
$$

$\bar{m}_{jk}$ and $\bar{p}_i$ are set equal to zero, since in practice they are difficult to realize and apply anyway. The final variational formulation of the MSG theory reads:

$$
\boxed{\int_V \left(\sigma_{ik}\delta u_{k,i} + p_i\delta u_{k,ki} + \mu^{(1)}_{ijk}\delta u_{k,ji} + \tfrac{1}{2}\epsilon_{jlk}\mu_{ij}\delta u_{k,li}\right)\mathrm{d}V = \oint_{\partial V}\bar{t}_k\delta u_k\mathrm{d}A}\ . \tag{16}
$$

3.2 Model implementation and boundary conditions

We follow a three-dimensional elasto-static finite element analysis of a cantilever beam (clamped on one side). Dirichlet boundary conditions are applied to the surface at $x = 0$, and a surface-traction vector $\bar{t}_k = (0, 0, \text{-}F/A)$ acts on the surface at $x = L$, where F and A are a single point force and the cross-sectional area of the beam, respectively, *cf.* Fig. (1). The Galerkin method is used for spatial discretization. The mesh consists of equidistantly distributed tetrahedral continuous Lagrange elements with a polynomial degree of two, corresponding to the order of the resulting partial differential equation (16). The system matrix is solved by using the method of Gaussian elimination (LU, for a lower/upper decomposition)

with low effort in time. The conventional elastic coefficients were chosen to be $E = 3.8$ GPa and $\nu = 0.38$, which are suitable for the material epoxy [11].

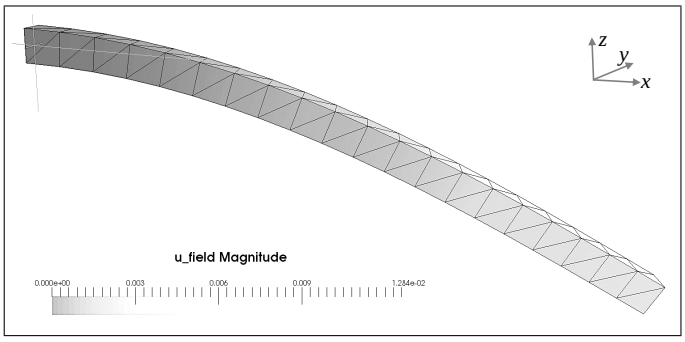

Figure 1: Mesh and deformation of a cantilever beam calculated in FeniCS©.

3.3 Analysis of the FE model

In a post-processing algorithm of the numerical solution, the present FE-model is analyzed regarding to the behavior of the higher-order stress measures presented in Eqn. (7). In addition to the deflection u_z we calculate the following quantities:

- the y-component of the rotation vector: $\varphi_y = \frac{1}{2}\epsilon_{yij}\, u_{j,i}$,
- an equivalent dilatation stress: $p_{\text{eqv}} = \sqrt{p_i p_i}$,
- an equivalent couple stress: $\mu_{\text{eqv}} = \sqrt{\mu_{ij}\,\mu_{ij}}$,
- an equivalent strain: $\varepsilon_{\text{eqv}} = \sqrt{\varepsilon_{ij}\,\varepsilon_{ij}}$,
- and an equivalent double-stress: $\mu^{(1)}_{\text{eqv}} = \sqrt{\mu^{(1)}_{ijk}\,\mu^{(1)}_{ijk}}$,

each along a line at $y = W/2$ and $z = T$ (cf. Fig. (2), (3) and (4)), where T is the thickness of the beam.

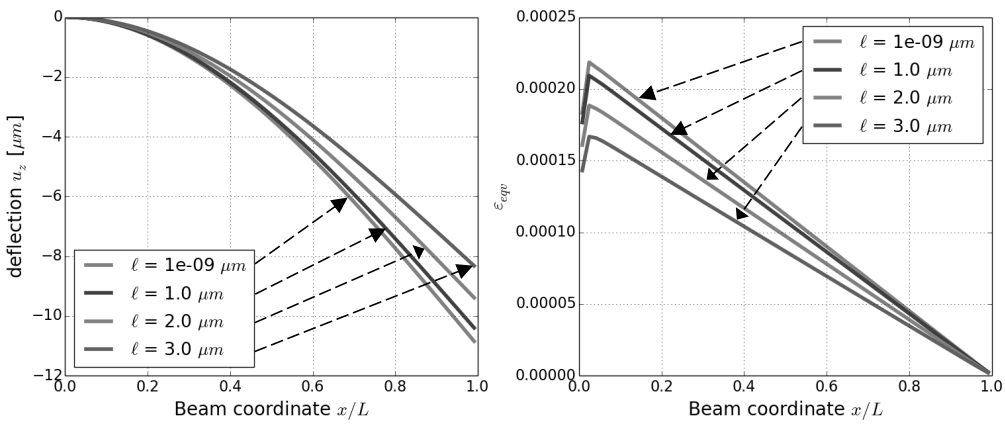

Figure 2: Deflections and equivalent strains along the line at $z = T$.

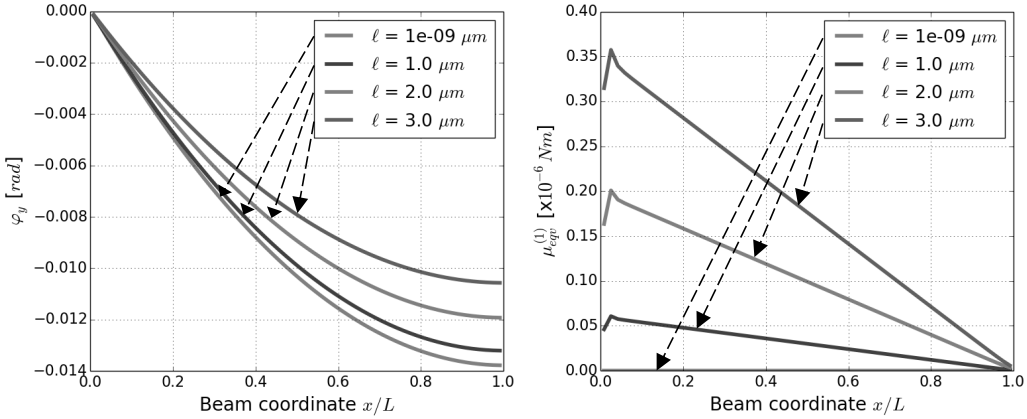

Figure 3: y-component of the rotation vectors and equivalent double-stresses.

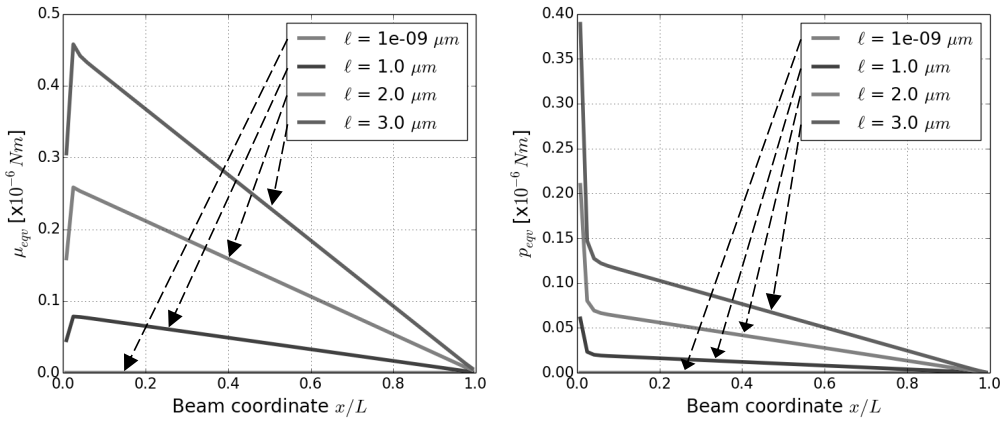

Figure 4: Equivalent couple stresses and equivalent dilatation stresses.

If ℓ is set equal to zero (ℓ=1x10^{-15} m), the solutions converge to the classical continuum solution, where there is no p_{eqv}, μ_{eqv}, and $\mu^{(1)}_{\text{eqv}}$. If ℓ is increased, u_z, φ_y and ε_{eqv} decrease, while the corresponding higher-order stress measures p_{eqv}, μ_{eqv}, and $\mu^{(1)}_{\text{eqv}}$ increase. The deviations close to the beam coordinate at $x=0$ in Fig's. (2), (3) and (4) are caused by a more complex stress state due to the boundary condition that is used for the clamped surface.

4 Experimental analysis

Static bending tests were performed on freestanding micro-beam structures made of epoxy. A load of $0.5 < F < 250$ µN was applied by using an off-axis laser-reflective Atomic Force Microscope (AFM) and deflections of 40 nm $< w <$ 10.0 µm were recorded. By assuming rectangular cross-sections of the specimens, the classical relation,

$$E^* = \frac{4L^3}{WT^3}\frac{F}{w} \ , \tag{17}$$

between the AFM measures (F/w) and the elastic modulus from the measurement E^* was used, where L is the length of the beam. The specimens had ratios of width to thickness of $W/T \approx$ 2–5 and length to thickness of $L/T \approx$ 15–40.

5 Results and conclusions

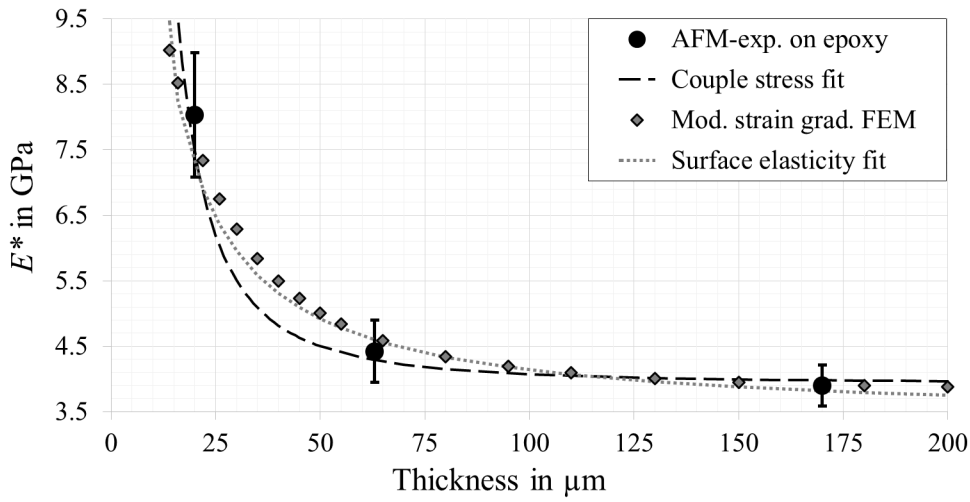

Figure 5: Results of the experiments, the couple stress model (Eqn. $(1)_1$), the surface elastic model (Eqn. $(1)_2$) and the finite element approach of the MSG theory

The results for the increasing elastic moduli are in very good agreement to the results of the couple stress and the surface elasticity analysis (both based on the Euler-Bernoulli assumptions) and to the AFM-experiments as well. The method of least squares gives the following values for the bulk elastic modulus and the corresponding additional material parameter: $E = 3.93$ GPa and $\ell = 7.75$ µm for the CS theory and $E = 3.37$ GPa and $E^{\text{surf}} = 1.3$ kN/m for the surface theory of elasticity. The FE-model for the MSG theory gives proper results in case of $E = 3.7$ GPa and $\ell = 7.9$ µm, see Fig. (5).

References

[1] Altenbach J., Altenbach H., Eremeyev V.A.: *On generalized Cosserat-type theories of plates and shells: A short review and bibliography.* Arch. Appl. Mech., **80**, pp. 73–92 (2010)

[2] Carpinteri A.: *Fractal nature of material microstructure and size effects on apparent mechanical properties.* Mechanics of Materials, **18**, pp. 89–101 (1994)

[3] Chong C.M.: *Experimental investigation and modeling of size effect in elasticity.* Dissertation, Hong Kong University of Science and Technology, 2002.

[4] Cuenot S., Fretigny C., Demoustier-Champagne S., Nysten B.: *Surface tension effect on the mechanical properties of nanomaterials measured by atomic force microscopy.* Physical Review B, **69**, pp. 01–05 (2004)

[5] Eringen A.C.: *A unified theory of thermomechanical materials.* Int. J. Engng. Sci., **4**, pp. 179–202 (1966)

[6] Eringen A.C.: *Continuum Physics. Vol. IV – Polar and nonlocal field theories.* Academic Press, INC. New York (1976)

[7] Eringen A.C.: *Nonlocal Continuum field theories.* Springer-Verlag, NY (2010)

[8] Fleck N.A., Muller G.M., Ashby M.F., Hutchinson J.W.: *Strain gradient plasticity: Theory and experiment.* Acta metall. mater., **42**(2), pp. 475–487 (1994)

[9] Fleck N.A., Hutchinson J.W.: *Strain gradient plasticity.* In: Hutchinson J.W., Wu T.Y. (Eds.), Adv. in Appl. Mech., **33**, Academic Press, NY, pp. 295–361 (1997)

[10] Gurtin M.E., Murdoch A.I.: *A continuum theory of elastic material surfaces.* ARMA, **57**(4), pp. 291–323 (1975)

[11] Lam D.C.C., Yang F., Chong C.M., Wang J., Tong P.: *Experiments and theory in strain gradient elasticity.* J. Mech. Phys. Sol., **51**(8), pp. 1477–1508 (2003)

[12] Li X.-F., Wang B.-L., Lee K.Y.: *Size Effect in the Mechanical Response of Nanobeams.* J. of Adv. Research in Mech. Eng., **1**(1), pp. 4–16 (2010)

[13] Liebold C., Müller W.H.: *Measuring material coefficients of higher gradient elasticity by using AFM techniques and Raman-spectroscopy.* In: Generalized continua as models for materials (Eds. Altenbach H., Forest S., Krivtsov A.), Advanced Structured Materials **22**, 2013, pp. 255–271.

[14] Logg A., Mardal K.-A., Wells G.N. et al.: *Automated solution of differential equations by the finite element method.* Springer, 2012, [doi:10.1007/978-3-642-23099-8].

[15] Ma Q., Clarke D.R.: *Size dependent hardness of silver single crystals.* Journal of Materials Research, **10**(4), pp. 853–863 (1995)

[16] McFarland A.W., Colton J.S.: *Role of material microstructure in plate stiffness with relevance to microcantilever sensors.* Journal of Micromechanics and Microengineering, **15**(5), pp. 1060–1067 (2005)

[17] Miller R.E., Shenoy V.B.: *Size-dependent elastic properties of nanosized structural elements.* Nanotechnology, **11**, pp. 139–147 (2000)

[18] Mindlin R.D., Eshel N.N.: *On first strain-gradient theories in linear elasticity.* International Journal of Solids and Structures, **4**, pp. 109-124 (1968)

[19] Nowacki W.: *Theory of micropolar elasticity.* CISM, Udine (1972)

[20] Salvetat J.-P., Kulik A.J., Bonard J.M., Briggs G.A.D., Stöckli T., Metenier K., Bonnamy S., Beguin F., Burnham N.A., Forró L.: *Elastic modulus of ordered and disordered multiwalled carbon nanotubes.* Adv. Mater. Weinheim, Ger., **11**, pp. 161165 (1999-b)

[21] Stan G., Ciobanu C.V., Parthangal P. M., Cook R.F.: *Diameter-dependent radial and tangential elastic moduli of ZnO nanowires.* Nano Letters, **7**(12), pp. 3691–3697 (2007)

[22] Yang F., Chong C.M., Lam D.C.C., Tong P.: *Couple stress based strain gradient theory for elasticity.* Int. J. of Sol. and Struct., **39**(10), pp. 2731–2743 (2002)

Christian Liebold, Wolfgang H. Müller
Berlin University of Technology, Faculty of Mechanics,
Chair of Continuum Mechanics and Materials Theory
Einsteinufer 5, 10587 Berlin, Germany